Single Quantum Dot Spontaneous Emission in a Finite-Size Photonic Crystal Waveguide: Proposal for an Efficient "On Chip" Single Photon Gun

V. S. C. Manga Rao and S. Hughes*

Department of Physics, Queen's University Kingston, Ontario K7L 3N6, Canada

(Received 4 July 2007; revised manuscript received 25 September 2007; published 7 November 2007)

Spontaneous emission rate enhancements from a single quantum dot embedded in a finite-size, planar photonic-crystal waveguide are investigated. Short waveguide lengths of only 10 to 20 unit cells are found to produce very large Purcell factors associated with a waveguidelike sharp resonance feature in the local density of photon states. Aided by theoretical insight and rigorous computational calculations, we explain the physics behind these remarkable emission enhancements and subsequently propose a ''single-photon gun'' with on-chip unidirectional collection efficiencies greater than 60% into an output wire waveguide. The advantages over recent proposals for infinitely long photonic-crystal waveguides are highlighted.

DOI: 10.1103/PhysRevLett.99.193901 PACS numbers: 42.55.Tv, 68.65.Hb, 78.67.Hc

Deterministic single-photon emitters, which seek to exploit the profound consequences of quantum mechanics to achieve unprecedented functionality, are currently one of the most sought after sources in quantum information science [1–5]. Two essential criteria for producing single-photon sources are (i) enhancing the spontaneous emission rates, so that decoherence effects are minimal, and (ii) efficient extraction and thus manipulation of the emitted photons. The first criterion of enhanced spontaneous emission (SE) can be achieved by placing a photon emitter in an environment that increases the local photon density of states (LDOS) through the Purcell effect [6]. This concept, along with the continued development in semiconductor fabrication technologies, has lead to a growing research field of semiconductor-based cavity quantum electrodynamics (cavity-QED) [7–9]. Cavity-QED regimes typically rely upon (quasi-) *closed cavity* systems, whereby one produces a standing-wave electric field in a cavity with a large quality factor Q and a small effective mode volume V_m. Therefore, when the cavity mode is resonant with the energy of the photon emitter, the SE can be modified. Less well studied is modified SE in an *open cavity* system, such as emission in a waveguide or photonic wire, though there have been several interesting predictions; e.g., Kleppner predicted in the early 1980s [10] that photon emission rates can be enhanced using cylindrical-wire waveguides for emission frequencies lying near the mode band edge.

The general concept of single-photon emission into a photonic wire is rich in physics and applications. The photonic wire, cf. a bar of silicon surrounded by air, uses the high-index-contrast to confine light at selected (e.g., telecommunication) wavelengths, using the principle of total internal reflection. By embedding a photon emitter at the center of such a photonic wire [11], fairly large collection efficiencies can be achieved (>50% into a bound propagation mode), though there is no SE enhancement which is necessary for solid-state single-photon emission applications (to overcome decoherence, e.g., caused by electron-phonon interactions). Photonic-crystal (PC) waveguides achieve much richer functionality by trapping light in the photonic band gap typically using air holes in a semiconductor slab, in which a waveguide channel is realized by removing an array of air holes. Consequently, Bragg diffraction can be exploited to achieve both enhanced SE and large collection efficiencies, though this enhanced functionality is considerably more complicated.

Recently, Hughes [12] demonstrated theoretically that large SE factors (>10) can be realized for single quantum dots (QD) embedded in a planar-PC waveguide, and some related results have been reported experimentally using leaky modes [13]. In addition, Lecamp *et al.* [14] and Manga Rao and Hughes [15] have also demonstrated that broadband (10 THz) single-photon β-factors of greater than 0.9 are achievable, where the single-photon β-factor is defined as the probability that an emitted photon will decay into a bound propagation mode [15]. The physical origin of enhanced SE decay in a PC waveguide is an arbitrarily large increase in the LDOS for slow-light modes near the photonic band edge. While such ''theoretical proposals'' [12,14,15] are attractive and timely with recent experiments, there remains a major problem associated with unavoidable fabrication imperfections that are now known to broaden any divergences in the expected LDOS. Even for so called *lossless* waveguide modes below the ''lightline'', propagation losses scale proportionally with the length of the waveguide and inversely with the mode group velocity [16–19]. Thus, the impact of imperfections for long waveguides will act to broaden the large SE factors and limit the proposed single-photon applications. In addition, it will be very difficult if not impossible to selectively embed only 1 single QD within a long waveguide, at the precise spatial and spectral position.

In an attempt to overcome these problems, in this Letter we study modified SE with a short finite-size PC waveguide of only 10 to 20 unit cells, with realistic boundary conditions similar to those that are always met in an experiment. In terms of efficient photon emission, our

scheme achieves close to the maximum-desired SE factors from single semiconductor QDs, while minimizing the problems of disorder-induced broadening and the technical difficulties of embedding only one QD at a field antinode in a long waveguide structure (typically thousands of unit cells). The maximum-desired SE factor is the enhancement than can be achieved before the onset of strong coupling, which is problematic for single-photon emission. In contrast to the infinite-length waveguide predictions [12,14,15], both the enhanced SE and large extraction efficiencies remain relevant to realistic samples, if they are finite size, even with a integrated coupler added. In addition to being a potentially useful framework for producing single photons, the proposed system gives rise to hitherto unexplored light-matter interactions, which allows one to probe the intriguing nature of photonic band gaps [20,21] in finite-size structures.

Proposal.—In Fig. 1(a) is shown a schematic of a finite-length planar-PC waveguide with a QD placed at the center of the slab. The PC material is expected to exhibit quasibound modes with spectral features similar to those of an infinite system, where light is trapped by the PC in the y direction, bound by total internal reflection in the z direction, and guided by the propagation Bloch modes in x. However, the precise nature of these modes is not known at all due to the termination of the lattice in the propagation direction. As a reference to our detailed analysis given below, in Fig. 1(b) we display the calculated band structure of the fundamental and higher order quasibound modes in an *infinite-length* planar-PC waveguide, lying within the TE-like band gap (the region between the dark gray areas). Below the air lightline these modes are bound and lossless (ignoring the impact of imperfections), while above the lightline the modes become intrinsically leaky when coupled to the continuum of radiation modes. The LDOS divergences (van Hove singularities) for emitter frequencies lying at the guided-mode band edge are expected, as the group velocity approaches zero. In what follows, we investigate single QDs that are positioned near the maximum of a field antinode in a finite-size PC. Two different structures are considered: (a) a planar-PC waveguide truncated with a definite number of unit cells and surrounded on either side by air, and (b) again a short PC waveguide but surrounded by air only on one end and closed by a *defect-free* PC on the other end (acting as a reflector). The planar PC is finite in all directions, though the infinite y-direction behavior is quickly realized after only a few unit cells of PC, and so one only needs a small finite number of holes in the y direction; thus most of the finite-size novelty stems from the propagation (x) direction. In addition, we also study the effect of adding an integrated wire-waveguide coupler [22,23].

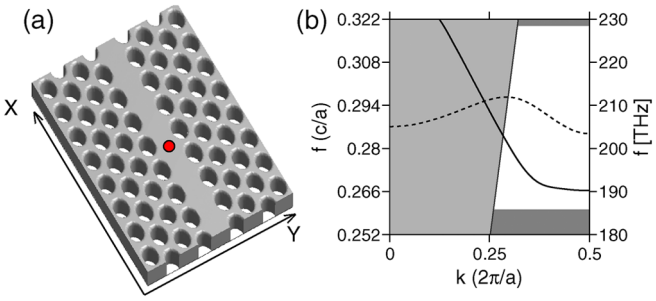

FIG. 1 (color online). (a) Schematic of a 10 unit-cell planar-PC waveguide (W1) along the x axis and a single quantum dot (QD: filled red circle) embedded at the center of the slab. The structure parameters used in the simulations are as follows: hole radius $r = 0.275a$, slab thickness $0.5a$, refractive index $n = \sqrt{12}$ and lattice constant $a = 420$ nm. (b) The band structure of modes (solid and dashed curves) corresponding to an infinite-length planar-PC waveguide [parameters as in (a)] shown within the TE-like band gap. The gray shaded region above the lightline represents the continuum of radiation modes.

Theory.—The theory of photon emission in an arbitrary surrounding can be made clear by first calculating the Green function tensor (GFT) [12,24–26]. Although this is in general a formidable task for finite-size structures, it can be determined in the usual way from a dipole solution of Maxwell's equations, whereby the electric-field GFT, $\mathbf{G}(\mathbf{r}, \mathbf{r}'; \omega)$, describes the field response at $\mathbf{r}'$ to an oscillating polarization dipole at $\mathbf{r}$, as a function of frequency. Once the GFT is known, it is a straightforward task to calculate the SE rates. For example, in the weak coupling regime of interest, the normalized SE factor ($\equiv F$) at the QD position ($\mathbf{r_d}$) is determined through

$$F(\mathbf{r_d}, \omega) = \frac{\mathbf{d} \cdot \mathrm{Im}[\mathbf{G}^{\mathrm{PC}}(\mathbf{r_d}, \mathbf{r_d}; \omega)] \cdot \mathbf{d}}{\mathbf{d} \cdot \mathrm{Im}[\mathbf{G}^{\mathrm{hom}}(\omega)] \cdot \mathbf{d}}, \qquad (1)$$

where $\mathbf{d}$ is a dipole moment of the QD electron-hole pair, and $\mathrm{Im}[\mathbf{G}^{\mathrm{hom}}]$ corresponds to that of the homogeneous bulk material with refractive index $n = \sqrt{\varepsilon}$, and $\mathbf{G}^{\mathrm{PC}}$ is the GFT of the PC. Since the semiconductor QDs of interest are disclike and much smaller than the size of a wavelength, only the in-plane polarization dipoles (x, y) are relevant and the dipole approximation can be employed. For an exciton energy level resonant with a cavitylike mode ($\omega_d = \omega_c$), and located at the field antinode ($\mathbf{r} = \mathbf{r_d} = \mathbf{r}_{\mathrm{anti}}$), the SE factor $F(\mathbf{r}_{\mathrm{anti}}, \omega_c) \approx 6\pi c^3 Q/[(\omega_c\sqrt{\varepsilon})^3 V_m]$. One can also calculate the "renormalized" response functions, such as the environment-modified relative permittivity of a QD, defined as $\Delta\varepsilon(\omega) = \Delta\varepsilon^0(\omega)/\{1 - V_d \mathrm{Im}[\mathbf{G}^{\mathrm{PC}}(\mathbf{r_d}, \mathbf{r_d}; \omega)]\Delta\varepsilon^0(\omega)\}$, where $\Delta\varepsilon^0(\omega) = |\mathbf{d}|^2/[2V_d\hbar\epsilon_0(\tilde{\omega}_d - \omega - i\gamma_{\mathrm{nr}}/2)]$, V_d is the volume of the QD, and γ_{nr} is the nonradiative decay rate. Note that $\tilde{\omega}_d \approx \omega_d$ can include a contribution from the Lamb shift (which comes from the real part of the GFT).

Calculations.—We stress that SE calculations for complex finite-size structures are considerably more complicated than that of infinite periodic systems. Consequently, to calculate $\mathbf{G}^{\mathrm{PC}}$ we have performed a direct numerical solution of the full 3D Maxwell's equations using finite-difference time-domain (FDTD) techniques [27]. Specifically, we excite a polarization dipole at the desired spatial

point and compute the total GFT directly, which is obtained for the finite-size sample. Beforehand, we first calculate the spatial profile of the fundamental waveguide mode [cf. Fig. 1(b)], and locate the antinode position of the y polarization field, near the center of the waveguide. This is the infinite waveguide solution, but gives us insight into what to first look for. We then excite the entire finite-size spatial domain with a y/x-polarized point dipole and calculate the appropriate elements of the GFT [$\mathbf{G}^{\mathrm{PC}}(\mathbf{r}, \mathbf{r}'; \omega)$]. In Figs. 2(a) and 2(b) are shown the calculated SE factors as a function of frequency for a 10 unit cell planar-PC waveguide bounded by, respectively, perfectly matched layers (PML) and an air medium on both ends for two different dipole orientations. The PML allows light to propagate out of the sample without any reflections, and in the x direction is included only as a useful reference. Remarkably, with only 10 unit cells, a comparison of the SE factors for both y- and x-oriented dipoles reveal all the essential features in the infinite-waveguide band structure, such as LDOS enhancements whenever the group velocity approaches zero (flat bands). With finite size, however, we note that the band-edge divergences are significantly broadened, and also the LDOS peaks are blueshifted from the ideal band structure (shown in the figure with a vertical dotted line). Moreover, when one includes air as a surrounding medium on both sides of the PC waveguide, there is a substantial enhancement of the SE factor (F) and there are additional spectral peaks arising due to Fabry-Perot resonances. For the LDOS peak indicated in Fig. 2(b), the corresponding y-polarized mode [x-polarized mode] at the center of the slab is shown as a contour image in Fig. 2(c) [Fig. 2(d)], which yields a calculated effective mode volumes of $V_m \approx 0.1\ \mu\mathrm{m}^3$. For comparison we note that the corresponding mode volumes of an infinite waveguide is about 0.01–0.02 $\mu\mathrm{m}^3$ per unit cell [15]. The mode profile shown dominates the GFT and the spatial dependence of the SE essentially follows the shape of the field modes ($\propto |E|^2$ which we have verified numerically). This suggests that QD spatial positioning to within 20–40 nm will be key in achieving the predicted large SE enhancements. We note that these large enhancements can be achieved for both x- and y-polarization components, although the peak frequencies will be different [cf. solid and dashed curves in Fig. 2(a)]. We remark that similar features in the PC waveguide LDOS have been obtained experimentally [28].

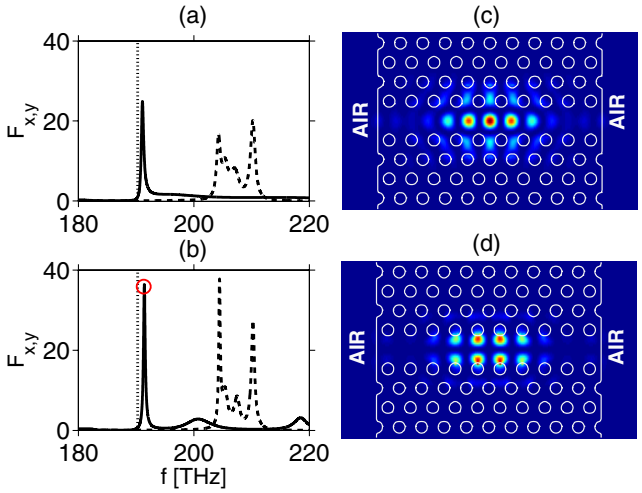

FIG. 2 (color online). (a) Spontaneous emission factors (F) versus frequency for a QD embedded in a 10 unit-cell finite-size waveguide surrounded by PML. Dashed (solid) line is for the case when the dipole orientation of the QD is along the $x(y)$ axis, and the dotted vertical line shows the band edge of the fundamental waveguide mode of an infinite structure. (b) Same as in (a) but with the waveguide ends surrounded by air. (c) Center of the slab contour of the $|E_y|^2$ field distribution corresponding to the peak Purcell factor shown in (b). (d) As in (c) but for the $|E_x|^2$ component of the E field.

Next, we study the effect of adding five layers of a regular PC to one end of the waveguide to act as a broadband mirror. This is expected to increase the SE while helping the emitted photon to travel only in one propagation direction. In Fig. 3(a) is shown the SE factors in a 10 unit-cell waveguide with air and a PC mirror on either side (solid curve); for a reference, the results for a waveguide with air on both sides are also shown (chain curve). As anticipated, we obtain an increase in F of up to 59 in the case of a PC mirror waveguide with a corresponding $Q \approx 1000$, in contrast to the air medium case which has a $F = 34$ with a corresponding $Q \approx 420$. Figure 3(b) displays the corresponding field profiles obtained at the fundamental LDOS peak [shown by a circle in Fig. 3(a)], from which we calculate $V_m \approx 0.144\ \mu\mathrm{m}^3$.

A key advantage of having a finite-size calculation of the SE factor is that one can investigate the sensitivity of the enhancements to the number of unit cells, which can then be matched in a systematic way to experiments. For example, in Fig. 3(c) is shown the SE factors for a 20 unit-cell waveguide demonstrating that very large SE factors up to 170–175 for an air medium and a PC mirror, are achievable with corresponding quality factors $Q \approx 7600$ and $Q \approx 6800$, respectively. The smaller adjacent peaks are again due to Fabry-Perot resonances caused by reflection from the PC-air interface. One also notices that in the case of longer waveguides, there is a spectral narrowing and a redshift in the resonances as compared to smaller guides. This behavior is not surprising since the LDOS and peak resonance frequency in longer waveguides must asymptotically converge to the band-edge of ideal infinite-length planar-PC waveguides (where the F is inversely proportional to the group velocity [12]). The field distribution $|E_y|^2$ for the 20 unit-cell PC mirror waveguide case is shown in Fig. 3(d). For single-photon applications one usually desires to maximize the SE while avoiding the regime of strong coupling. As shown in the insets of Figs. 3(a) and 3(c), for a QD dipole strength of $|\mathbf{d}| = 50$ D (dashed curve), both the 10 and 20 unit-cell waveguide with a PC mirror give close to the maximum desired SE factor for single-photon emission; in contrast, for a larger dipole

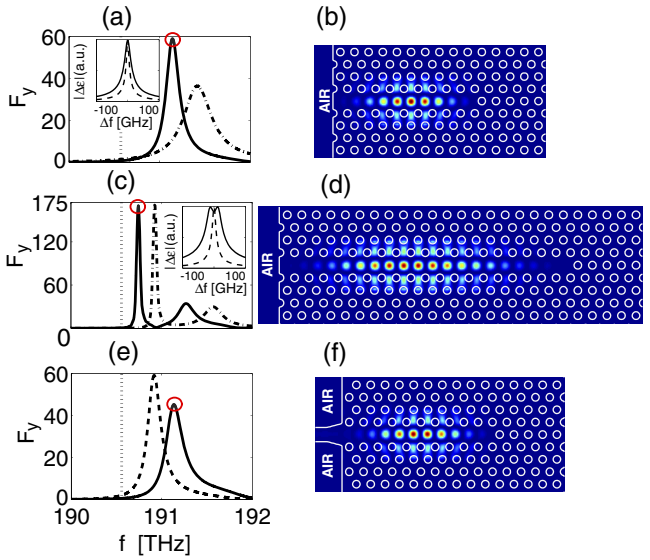

FIG. 3 (color online). (a) A comparison of the SE factor (F) versus frequency for a QD embedded in a 10 unit-cell sized planar-PC waveguide with both ends surrounded by air (chain curve), and with one end of the waveguide surrounded a regular PC (solid curve); the dotted vertical line shows the band edge of the fundamental waveguide mode of an infinitely long structure; the inset shows the QD permittivity for two different dipole moments (see text). (b) Center of the slab contour of the $|E_y|^2$ field distribution corresponding to the peak SE factor shown in (a) with a circle. (c),(d) Same as in case (a),(b) but with 20 unit-cell waveguide. (e) A comparison of SE factors in the case of 10 unit-cell sized PC mirror waveguide with different boundaries. PML surroundings (dashed line) and a wire-waveguide coupler (solid line). (f) Same as (b) but with a wire-waveguide output coupler.

moment, e.g., 100 D (solid curve), then only the 10 unit cell (smaller waveguide) remains suitable as a single-photon source, since the 20 unit-cell waveguide already yields strong-coupling (cf. the spectral doublet in the QD permittivity response). We next add in an integrated wire waveguide-coupler (non-PC), which is known to efficiently couple to a fiber [23], and example the case of 10 unit cells only [cf. Figs. 3(e) and 3(f)]. While the presence of the coupler (solid curve) reduces F, the overall SE enhancement is still very significant.

Finally, we address the important issue of photon extraction. For the case of a waveguide surrounded by air on both sides, the collection efficiency in the x direction for a 10 (20) unit-cell waveguide is 26.% (27.5%) in either direction ($\pm x$) for air on both sides, with the rest being lost to vertical leakage. However, with a PC mirror, the collection efficiency for a 10 (20) unit-cell waveguide in a unidirectional output (i.e., $-x$ direction, to the left) is 53% (52%). More importantly, with the integrated coupler, more than 60% of coupling into the output waveguide mode is estimated (this also includes a mode-overlap calculation), which can easily be integrated with an output fiber coupler [23]. For larger waveguides such as with 20 unit cells, this output coupling was actually found to decrease, signaling that more light is lost vertically for longer waveguides, even for an ideal structure. Although we have not yet tried to optimize the material parameters, we anticipate that with suitable design, optimum SE factors for single photon emission can be achieved with a simultaneous 70%–80% output coupling efficiency.

In conclusion, we have studied the physics of single-QD photon emission from finite-size PC waveguides and proposed a miniaturized device that merits investigation for single-photon emission applications "on chip." Very large SE factors are obtained, and efficient unidirectional output is achieved using a PC mirror and an integrated output coupler. The single-photon emitter is expected to be robust with respect to fabrication disorder and is small enough to allow deterministic positioning of a single QD.

This work was supported by the National Sciences and Engineering Research Council of Canada and the Canadian Foundation for Innovation.

*shughes@physics.queensu.ca

[1] E. Moreau *et al.*, Appl. Phys. Lett. **79**, 2865 (2001).
[2] D. Fattal *et al.*, Phys. Rev. Lett. **92**, 037904 (2004).
[3] N. Yoran and B. Reznik, Phys. Rev. Lett. **91**, 037903 (2003).
[4] A. Beveratos *et al.*, Phys. Rev. Lett. **89**, 187901 (2002).
[5] B. Lounis and M. Orrit, Rep. Prog. Phys. **68**, 1129 (2005).
[6] E. M. Purcell, Phys. Rev. **69**, 681 (1946).
[7] M. Pelton *et al.*, Phys. Rev. Lett. **89**, 233602 (2002).
[8] T. Yoshie *et al.*, Nature (London) **432**, 200 (2004).
[9] K. Hennessy *et al.*, Nature (London) **445**, 896 (2007).
[10] D. Kleppner, Phys. Rev. Lett. **47**, 233 (1981).
[11] G. Lecamp *et al.*, Proc. SPIE **6195**, 61 950(E) (2006).
[12] S. Hughes, Opt. Lett. **29**, 2659 (2004).
[13] E. Viasnoff-Schwoob *et al.*, Phys. Rev. Lett. **95**, 183901 (2005).
[14] G. Lecamp *et al.*, Phys. Rev. Lett. **99**, 023902 (2007).
[15] V. S. C. Manga Rao and S. Hughes, Phys. Rev. B **75**, 205437 (2007).
[16] S. Hughes *et al.*, Phys. Rev. Lett. **94**, 033903 (2005).
[17] E. Kuramochi *et al.*, Phys. Rev. B **72**, 161318 (2005).
[18] M. L. Povinelli *et al.*, Appl. Phys. Lett. **84**, 3639 (2004).
[19] D. Gerace and L. C. Andreani, Opt. Lett. **29**, 1897 (2004).
[20] E. Yablonovitch, Phys. Rev. Lett. **58**, 2059 (1987).
[21] S. John, Phys. Rev. Lett. **58**, 2486 (1987).
[22] E. Miyai and S. Noda, J. Opt. Soc. Am. B **21**, 67 (2004).
[23] M. G. Banaee *et al.*, Appl. Phys. Lett. **90**, 193106 (2007).
[24] P. Lodahl *et al.*, Nature (London) **430**, 654 (2004).
[25] H. T. Dung *et al.*, Phys. Rev. A **62**, 053804 (2000).
[26] O. J. F. Martin *et al.*, Phys. Rev. Lett. **82**, 315 (1999).
[27] We use FDTD Solutions, see: www.lumerical.com.
[28] X. Letartre *et al.*, Appl. Phys. Lett. **79**, 2312 (2001).